TRIBOLOGIA - Finnish Journal of Tribology 3-4 vol 38/2021

https://doi.org/10.30678/fjt.97530

SUOMEN TRIBOLOGIAYHDISTYS RY
THE FINNISH SOCIETY FOR TRIBOLOGY
www.tribologysociety.fi
https://journal.fi/tribologia

Study on Solid Particle Erosion of Pump Materials by Fly Ash Slurry using Taguchi's Orthogonal Array

Jashanpreet Singh[1], Satish Kumar[2], S. K. Mohapatra[1]
[1]Department of Engineering, Punjab State Aeronautical Engineering College, Patiala 147001, Punjab, India
[2]Department of Mechanical Engineering, National Institute of Technology, Jamshedpur 831014, Jharkhand, India
Corresponding author: Jashanpreet Singh (jashanpreet.singh@mrsptu.ac.in)

ABSTRACT

Various grades of stainless steel are used to fabricate the pump impeller, casings, and seals used in heavy-duty erosion and corrosion conditions. In the present study, stainless steel (SS316L, SS304, SDSS2507) and grey cast iron used in the fabrication of heavy-duty pump impellers were taken for the analysis of solid particle erosion. Experiments were conducted on the lab-scale slurry pot tester. Fly ash slurry was prepared of different concentrations (wt%). Taguchi's orthogonal array is used to design the experiments of erosion wear for the variation of rotational speed, solid concentration, time, and particle size. Results showed that SS316L showed superior microhardness and wear behavior against the fly ash slurry followed by SS304, SDSS2507 and Grey cast iron.

Keywords: Erosion wear, slurry erosion, pump materials, slurry pump, design of experiments.

1. INTRODUCTION

Nowadays, almost every engineering field is facing the problem of protecting the machinery from different types of damage or failures [1]. The protection of various industrial machines, equipment, and systems is recognized by many engineers, researchers, and scientists. It requires a high level of process-based understanding that involves in the economic solution of such failure problems. The market of materials has grown at a high level at present time. A variety of materials are available which can withstand different forces such as tensile force, compressive force, impact loading, fatigue loading, etc. [1-3]. However, the degradation processes are found to be more aggressive for pump materials in hydraulic slurry conditions than other forces. So, the selection of material becomes a formidable task from the concern of performance, maintenance, and economy. The selection of materials is an essential part of controlling erosion wear. In the different Industries, the solids extracted by slurry pumps are unique in terms of nature [4-7].

Erosion wear is the material deterioration process that occurs due to the continuous impingement of solid slurry particles [8-11]. Erosion wear takes place by the relative motion between slurry particles and solid surfaces through the erosive action. Solid particles strike the material surface and surface failure take place either by directional impact or random-collisions [12]. A large number of parameters contribute to the erosion wear phenomenon like the velocity of flowing media, time, slurry concentration, angle of impingement, properties of the material used for fabrication, etc. [13]. The mining conditions are the most severe for the materials. Such conditions become more dangerous during the accelerated environment. The accelerated environment is imposed while the fast-moving particles strike the materials at high velocities such as pump casings, impellers, nozzles, valve seats, tubes, tees, flanges, elbows, etc. [14, 15].

In present investigation, four different pump materials like stainless steel (SS316L, SS304, SDSS2507) and grey cast iron are selected. Such materials are used globally in the manufacture of various slurry pump parts. For certain cases, the key justification for choosing such materials was their versatility, excluding slurry pumps, such as turbine blades, slurry pipes, elbows, and so on. The present research aims to study the erosion of pump materials used in the thermal power plant's slurry transport system which conveys fly ash. The orthogonal array of Taguchi's method is used to conduct the erosion experimentation for the variation in rotational speed, concentration, time, and particle size.

2. MATERIALS AND METHODS

2.1 Pump materials

The grey cast iron (G.C.I.) is widely used to fabricate the pump casings. Cast iron is cheap and commercially available in the market and is also known for its high hardness. Stainless steels namely SS304 and SS316L are

TABLE 1. Compositional analysis of different pump materials.

Material	Elements (%)										
	S	P	C	Mo	Mn	Si	Ni	Cr	Co	N	Fe
SS316L	0.005	0.083	0.005	1.690	1.020	0.1350	10.350	16.600	1.690	---	Bal.
SS304	0.025	0.015	0.08	---	3.640	0.31	7.960	18.040	---	---	Bal.
SDSS2507	0.011	---	0.0350	3.960	---	---	5.990	23.980	---	0.210	Bal.
Grey Cast iron	0.200	0.880	3.430	----	0.550	3.360	---	---	---	---	Bal.

widely used as pump materials for the fabrication of the impeller, casings and seals. In heavy-duty erosion and corrosion conditions, super duplex stainless steels are widely used. In the present study, super duplex stainless steel (SDSS2507) was used which has application in the fabrication of heavy-duty pump impellers. SS316L and SS304 were purchased from Pearl Overseas, Mumbai (Maharashtra, India). SDSS2507 was purchased from Jayant Ferromet LLP, Mumbai (Maharashtra, India). The metallographic analysis was performed before erosion wear experiments using the optical emission spectrometer (Foundry master, Oxford Instruments, Uedem, Germany), as summarized in Table 1.

2.2 Testing specimen

For experiments, the dimensions of the specimen were kept as 67.5×25.4×6.35 mm with a central hole of 8.5 mm diameter for fixing it in the equipment's spindle. The schematic diagram of the sample specimen is presented in Fig. 1. The shape of the specimen was taken as per the standard recommended for the instrument by Ducom instruments, Bangalore (India).

2.3 Erodent particles

Fly ash was collected from electrostatic precipitators of location GGSS Thermal Power Plant, Ropar, India. Fig. 2 presents the scanning electron microscopy (SEM) and X-ray Diffractometry (XRD) images of the fly ash. The particles of fly ash seem spherical. XRD pattern depicted that quartz (SiO_2), mullite ($Al_{4.62}Si_{1.37}O_{9.65}$), hematite ($Fe_2O_3$), and kyanite ($Al_2SiO_5$) crystalline phases were present in fly ash. The minor peaks of Fe_2O_3 were observed that represents its small proportion in fly ash.

2.4 Microhardness testing

A Metatech MVH-1, Pune, India microhardness tester was employed to test the microhardness (HV1) with the help of a Vickers indenter. The indentation load during the study was taken as 1000 g (1 kg).

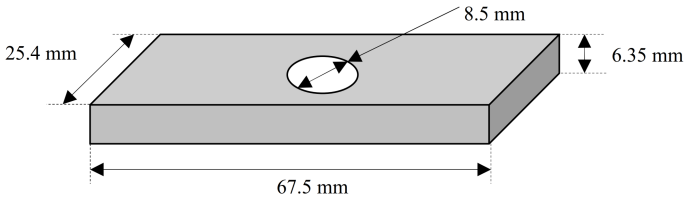

FIGURE 1. Schematic diagram of specimen's geometry.

3. EXPERIMENTS

3.1 Taguchi's orthogonal array

The design of experiment (DOE) was implemented for optimization of erosion wear of pump materials. Generally, the erosion wear parameters can't be optimized because erosion wear problem is directly associated with the increase or decrease of a particular parameter. Minimum the value of influencing parameters results in the minimum value of erosion wear. According to the objective of present study, it is important to identify the most influential parameter amongst from different parameters. In this context, Taguchi's method was used to identify the most influencing parameter [16-18]. Erosion wear (in g/m^2) was evaluated by measuring the weight loss (in g) per unit area (m^2) of the specimen with the help of an electronic weighing machine of least count 10^{-4} gram. L_{16} (4^2) orthogonal array was used for five input parameters and each of parameter has four levels as listed in Table 2. The rotational speed was adjusted to obtain the velocity of particles in the range of 1 to 5 m/s. Weight loss from the specimen was chosen as an output criterion. Experiments were performed as per the recommendations made by Desale et al. [13].

3.2 Slurry preparation

A fixed volume of tap water was added to achieve the required stable slurry suspension of fly ash particles. The slurry was rendered in a 2000 ml cylindrical pot and stirring for 30 minutes at a rate of 350 rev min. The weighing of solid and liquid was done by using an electron weighing machine having the least count of 0.05 kg. The

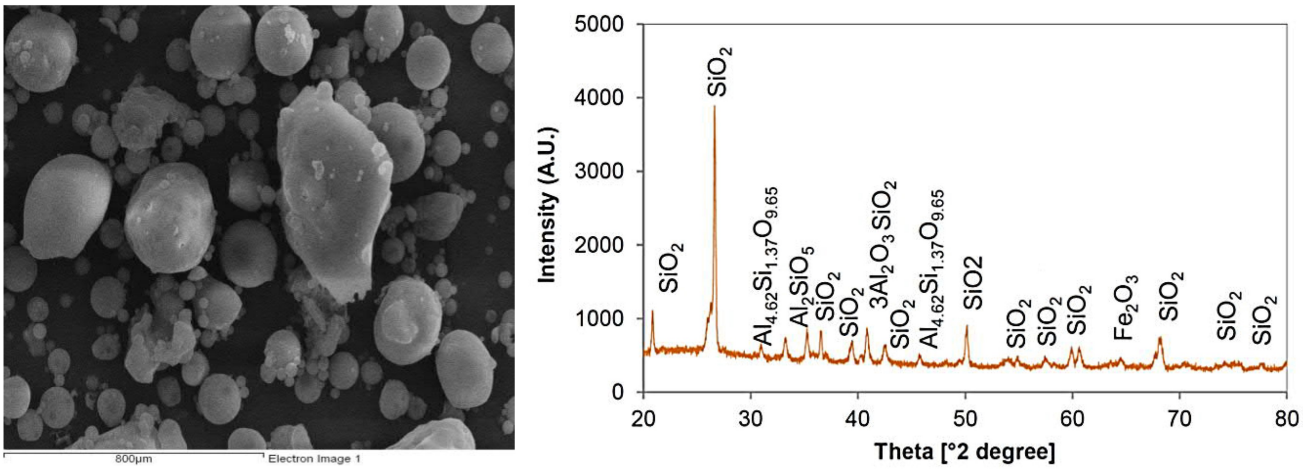

(a) (b)

FIGURE 2. (a) Scanning electron microscopy i.e. SEM, and (b) X-ray Diffractometry i.e. XRD images of fly ash.

average fineness number (AFN) of fly ash particles was calculated by using the following empirical formula:

$$AFN = \frac{\sum\left(Mi \times \left(m_i \times g\right)\right)}{\sum\left(m_i \times g\right)} \quad (1)$$

Where the g is equal to the gravity i.e. 9.81 m/s. Summation of m_i is the sum of masses retained in each sieve, and M_i represents the British sieve standard (BSS) multiplier.

3.3 Testing equipment

The wear tests were conducted on the tested pot tester, Model: TR-401, Ducom instruments, Bangalore, India. The experiments performed by this tester are helpful in prediction the wear of pump impeller, casing, and slurry pipelines. The erosion wear pot tester (along with components) used in the present study is shown in Fig. 3. The size of the cylindrical pot was 120 mm × 120 mm (internal diameter × height). A Digital meter on a controller unit was given, which regulates the speed of the spindle. The circulation of water in the cooling vessel around the pot removes the heat generated during experiments. The screw jack placed to the pot's bottom adjusts its height. The specimen was screwed in the propeller shaft shown in Figure 3. The specimen was positioned such as the distance between specimen and pot remains as 10 mm. The pot was filled with the slurry of specific solid concentration according to the set of experiments.

4. RESULTS AND DISCUSSIONS

4.1 Surface microhardness analysis

The testing of microhardness was performed in a total of six trials for producing the experimental repeatability. The average microhardness of the SS304, SS316L, SDSS2507, and grey cast iron was found as 237±5.5, 296±11.0, 212±2.5, and 207±3.5 HV1 respectively.

TABLE 2. Variable parameters of different experiments.

S. No.	Factors	Levels			
		I	II	III	IV
1	Speed (rev/min)	600	900	1200	1500
2	Time (min)	90	120	150	180
3	Concentration (wt%)	30	40	50	60
4	Material	G.C.I.	SS304	SS316L	SDSS2507
5	Average fineness number (µm)	30.9	89.3	120.4	184.5

4.2 Signal-to-noise ratio

The experimental output was converted with a MINITAB 18 tool in terms of signal-to-noise (S/N) ratios. The S/N ratio depends upon the performance characteristics. The difference between S/N ratios decides the most affecting parameter. In present work, the lower-the-better quality rule was employed to calculate the value of S/N ratio for output (y) in 'n' number of observations:

$$S/N = -10 \times \log\left[\frac{1}{n}\Sigma\, y_i^{\,2}\right] \quad (2)$$

In the present study, the value of 'n' was 16.

Fig. 4 shows the mean effect of S/N ratios of erosion wear generated by fly ash slurry. However, the average fineness number varies in the case of fly ash. The average fineness number of fly ash slurry (AFN) was measured as 30.9, 89.3, 120.4, and 184.5 µm respectively for the particle size range of <75, 75-106, 106-150, and >150 µm. The size of fly ash particles was measured before experiments. From Fig. 4 and Table 3, the S/N ratio for parameters namely

FIGURE 3. Photograph of the erosion wear pot tester.

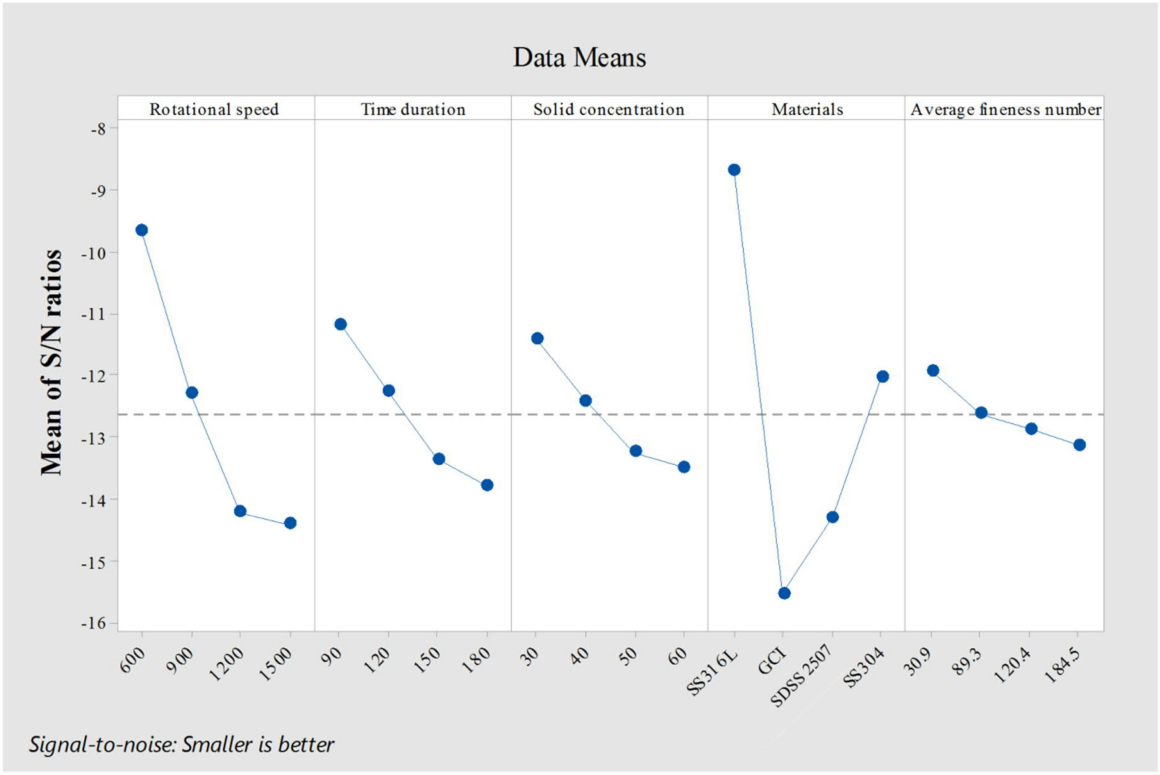

FIGURE 4. Main effect plot for S/N ratios of erosion wear generated by fly slurry.

average fineness number, rotational speed, test duration, and solid concentration was found to decrease with an increase in erosion wear. The erosion wear was observed to increase with increased speed, concentration, time, and AFN. It was found that the erosion wear increases with an increase in rotational speed, test duration, solid concentration (wt%), and AFN. The reason behind the increase of erosion wear with speed is that the particles' kinetic energy is directly associated with the speed of the propeller shaft. Higher the kinetic energy of fly ash particles tends toward the high impact energy during the interaction between specimen and particles [13]. Thus, the higher erosion occurs with the increase of speed of the tester. Furthermore, the solid concentration of particles involves in the particle-specimen interaction phenomenon. A large number of interactions increases the erosion wear [7]. Particle-specimen interaction phenomenon generally promoted with the presence of the number of particles, as a result, erosion increases. However, the AFN is directly propositional to the average size of particles. As the particle size increases, the areas of the impact made by particles with specimen surface increases hence, the larger particles damage more surface area.

However, the order of S/N ratio for erosion wear of different materials was found as Grey cast iron > SDSS2507 > SS304 > SS3136L. The low value of the S/N ratio of erosion wear of SS316L shows its minimum erosion wear as compared to SS304, SDSS2507, and grey cast iron. Grey

TABLE 3. S/N ratios for erosion wear at different input parameters for fly ash slurry.

S. No.	Rotational speed, rev/min	Time, min	Concentration, wt%	Materials	AFN, µm	Erosion wear, g/m²	S/N ratio
1	600	90	30	SS2507	30.9	2.492	-7.932
2	600	120	40	GCI	89.3	3.955	-11.943
3	600	150	50	SS304	120.4	3.391	-10.606
4	600	180	60	SS316L	184.5	2.564	-8.178
5	900	90	40	SS304	184.5	3.343	-10.483
6	900	120	30	SS316L	120.4	2.234	-6.980
7	900	150	60	SS2507	89.3	5.943	-15.480
8	900	180	50	GCI	30.9	6.480	-16.232
9	1200	90	50	SS316L	89.3	2.945	-9.382
10	1200	120	60	SS304	30.9	4.661	-13.370
11	1200	150	30	GCI	184.5	7.165	-17.104
12	1200	180	40	SS2507	120.4	7.099	-17.024
13	1500	90	60	GCI	120.4	7.111	-16.915
14	1500	120	50	SS2507	184.5	6.922	-16.805
15	1500	150	40	SS316L	30.9	3.254	-10.248
16	1500	180	30	SS304	89.3	4.842	-13.701

cast iron shows maximum erosion wear among these parameters which may be due to the low microhardness than other materials. Furthermore, the graphite flakes appeared on the surface of grey C.I. which contributes to ease of plastic deformation at the edges of flakes.

From Table 3, the value of erosion was observed maximum as 7.16 g/m² at N = 1200 rev/min, T = 150 min, C_w = 30% and AFN = 184.5 µm for grey cast iron. Erosion wear was found minimum as 2.234 g/m² at N = 900 rev/min, T = 120 min, C_w = 30% and AFN = 120.4 µm for SS316L. This also indicates the same trend of erosion wear for materials. From mean effect plots, it is very tough to analyze the most influencing parameter due to close values of S/N ratios. Thus, it needs further analysis to reveal the most influencing factor as well as the relationship between various parameters.

4.3 Response of parameters

The rank and delta values have been calculated based on the quality rule of S/N ratios (i.e. smaller-the-better). Table 4 lists the responses of different S/N ratios to erosion damage through fly ash slurry. The value of delta in the response table of erosion wear by fly ash slurry was found as 6.851, 4.752, 2.606, 2.057, and 1.197 respectively for material type, speed, concentration, time, and AFN. The higher value of delta represents the higher rank of a particular factor. From the calculated data, the rank of material type was observed highest among rotational speed, test duration, solid concentration (wt%), and AFN. Among process parameters, the rotational speed was the most influencing factor. The results data validates the statement of researchers [10, 19]. From values of the response of material type, it was also found that SS316L had shown minimum erosion wear as compared to SS304, SDSS2507, and grey cast iron.

The relationships between erosion wear and parameters are shown in Fig. 5. Parallel and nonparallel lines can be visualized due to the absence of and existence of parametric communication respectively. It looks as though there have been substantial wear with increasing speed over time, solid concentration, AFN, and material type. However, neither line is parallel to the other line in all

TABLE 4. Response table for S/N ratios for erosion wear by fly ash slurry.

Level	Rotational speed	Test duration	Solid concentration	Materials	Average fineness number
1	-9.665	-11.178	-11.429	-8.697	-11.945
2	-12.294	-12.275	-12.424	-15.548	-12.626
3	-14.220	-13.359	-13.256	-14.310	-12.882
4	-14.417	-13.784	-13.486	-12.040	-13.142
Delta	4.752	2.606	2.057	6.851	1.197
Rank	2	3	4	1	5

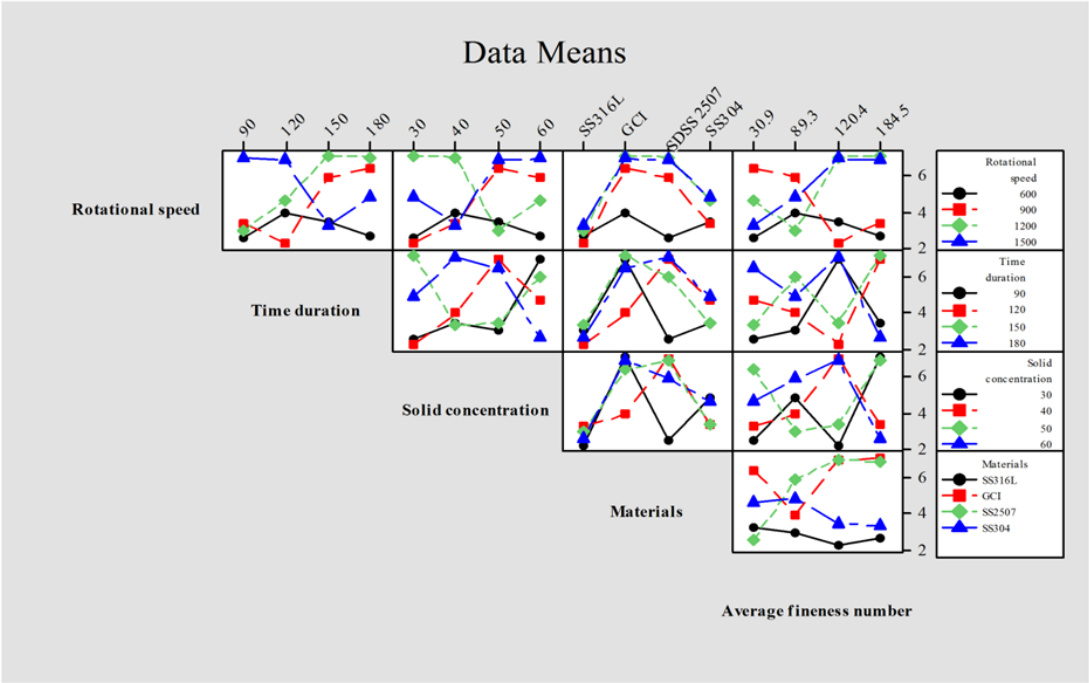

FIGURE 5. Interaction plot between different parameters for erosion wear by fly ash slurry.

figures which show that time-concentration, times-AFN, and concentration-material are significantly interactive. Blue lines can also be seen crossing the other lines significantly. This implies that the avg. amount of various determining factors was the source of major erosion.

4.4 Microstructural analysis of wear mechanisms

For the microstructural analysis, the scanning electron microscopy was performed for the eroded surfaces (at a solid concentration of 30%, a rotational speed of 1500 rev/min, impact angle of 0°, test duration of 180 min). The impact angle becomes 0° in this pot tester while the test specimen was fixed in the spindly at 0°. However, the SEM images were taken at longitudinal ends of the specimen, where the maximum wear occurred. Fig. 6(a) indicates the SEM pictures of SS316L after experiments of erosion by fly ash. From the SEM image (Fig. 6a), the wear of fly ash erosion contributed to micro-cutting results. Also, the ploughed and cratered area can be seen frequently in the SEM image however, the minor area seems to be cratered. Similarly, the surface morphology of SS304 eroded surface by fly ash slurry is shown in Fig. 6(b). A large region shows the microcutting action on the surface of SS304. Surface morphology and topology of SDSS2507 eroded surface by fly ash slurry are shown in Fig. 6(c). From Fig. 6(c), the ploughing and microcutting action were observed on the surface of SDSS2507. Few regions were undergone microcutting actions. Similarly, the surface morphology of Grey C.I. eroded surface by fly ash slurry is shown in Fig. 6 (d). Grey cast iron (C.I.) shows different erosion wear behavior as compared to the stainless steels. Grey C.I. contains graphite flakes that underwent craters mechanism. The ductile erosion wear occurs while a material undergoes plastic deformation as a primary mechanism which leads to plouging, lip formation, and craters [8, 11]. On the other hand, the material undergoes

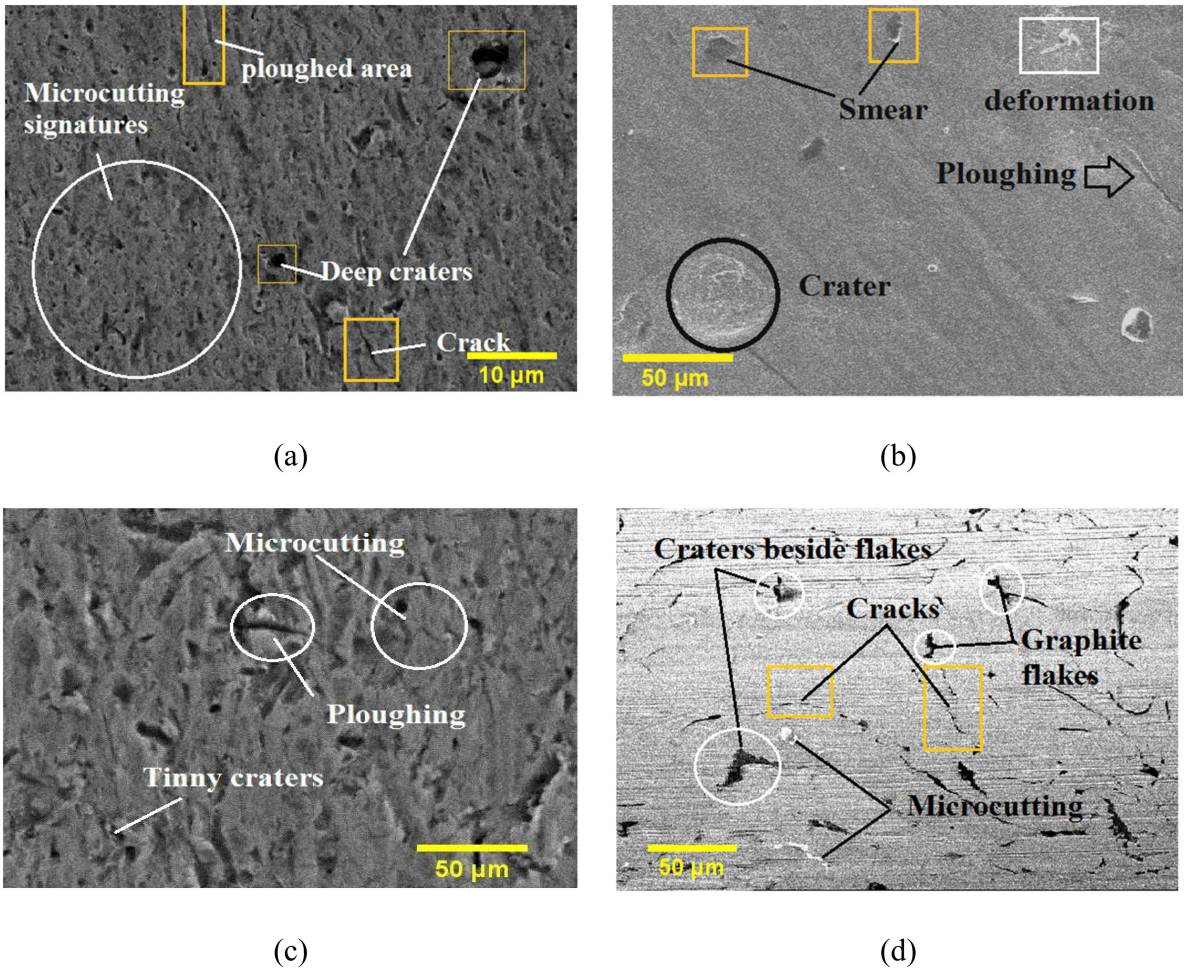

FIGURE 6. Surface morphology of (a) SS316L, (b) SS304, (c) SDSS2507, and (d) Grey cast iron eroded surface by fly ash slurry.

microcutting in brittle erosion mechanism and follows the fractures, cracking, and debonding as secondary mechanisms [9].

5. CONCLUSIONS

The present research aims to study the erosion of pump materials used in the thermal power plant's slurry transport system which conveys fly ash. Following conclusions are drawn based on the present study:

- The order of S/N ratio for erosion wear of different materials was found as; Grey cast iron > SDSS2507 > SS304 > SS3136L.
- The most influencing factor is material type amongst speed, time, concentration (wt%), and average fineness number.
- The average microhardness of the SS316L (before the experiments) was found higher amongst all materials used in this study and followed by SS304, SDSS2507, and grey cast iron. High hardness of SS316L strengthens it against erosion conditions.
- Microscopically, the SEM images of SS316L showed the mechanisms like micro-cutting, ploughing, and craters. However, the surface morphology of eroded SS304 presents a large region that underwent microcutting action whereas the eroded SDSS2507 surface showed ploughing, tinny craters, and microcutting mechanisms.
- Eroded grey cast iron showed different erosion wear behavior as compared to the stainless steels. Grey cast iron containing graphite flakes underwent craters and cracking.
- The wear mechanisms highlight the ductile erosion wear phenomenon of stainless steels used in the present study whereas grey cast iron presents the brittle erosion wear phenomenon.

Acknowledgments

This work has not received any funding directly/ indirectly from any institution/university, agency, or organization.

References

1. J. Singh, "Investigation on slurry erosion of different pumping materials and coatings," Ph.D. thesis, Thapar Institute of Engineering and Technology,

Patiala, India, 2019.

2. K. Kato, and K. Adachi, "Wear Mechanisms," in Modern Tribology Handbook, edited by B. Bhushan (CRC Press, Boca Raton, 2001), pp. 28.https://doi.org/10.1201/9780849377877.ch7
3. J. Singh, S. Kumar, S.K. Mohapatra, Proceed. IMeche Part J: J. Eng. Tribol 233, 712-725 (2019). https://doi.org/10.1177/1350650118794698
4. J. Singh, S. Kumar, S.K. Mohapatra, Ceramic. Int. 45, 23126-23142 (2019). https://doi.org/10.1016/j.ceramint.2019.08.007
5. V. Javaheri, D. Porter, V.-T. Kuokkala, Wear 408-409, 248-273 (2018). https://doi.org/10.1016/j.wear.2018.05.010
6. C.N. Machio, G. Akdogan, M.J. Witcomb, S. Luyckx, Wear 258, 434-442 (2005). https://doi.org/10.1016/j.wear.2004.09.033
7. J. Singh, S. Kumar, S.K. Mohapatra, Indust. Lub. Tribol. 71(4), 610-619 (2019). https://doi.org/10.1108/ILT-04-2018-0149
8. I. Finnie, Wear 3, 87-103 (1960).https://doi.org/10.1016/0043-1648(60)90055-7
9. J.G.A. Bitter, Wear (6), 5-21 (1963).https://doi.org/10.1016/0043-1648(63)90003-6
10. B.K. Gandhi, S.N. Singh, V. Seshadri, Tribol. Int. 32, 275-282 (1999). https://doi.org/10.1016/S0301-679X(99)00047-X
11. B.K. Gandhi, S.N. Singh, V. Seshadri, J. Fluid. Eng. 123, 271-280 (2001). https://doi.org/10.1115/1.1366322
12. M.C. Roco, and G.R. Addie, Powder Technol. 50, 35-46 (1987). https://doi.org/10.1016/0032-5910(87)80081-5
13. G. R. Desale, B.K. Gandhi, S.C. Jain, Wear 259, 196-202 (2005). https://doi.org/10.1016/j.wear.2005.02.068
14. M. Szala, and L. Daniel, J. Technol. Exploit. Mech. Eng. 2, 40-44 (2016). https://doi.org/10.35784/jteme.337
15. E. Rabinovich, and H. Kalman, Review. Chem. Eng. 27, 215-239 (2011). https://doi.org/10.1515/REVCE.2011.011
16. G. Taguchi, Introduction to Quality Engineering, Tokyo. Asian Production and Organization, Tokyo (1990).
17. B. Stojanovic, J. Blagojević, M. Babic, S. Veličković, S. Miladinovic, Indust. Lub. Tribol. 69, 1005-1015 (2017).https://doi.org/10.1108/ILT-02-2017-0043
18. S. Veličković, B. Stojanović, M. Babić, I. Bobić, J. Compos. Mater. 51, 2505-2515 (2017). https://doi.org/10.1177/0021998316672294
19. R. Gupta, S.N. Singh, V. Sehadri, Wear 184, 169-178 (1995). https://doi.org/10.1016/0043-1648(94)06566-7